Korean J. Chem. Eng., **31**(1), 12-19 (2014)
DOI: 10.1007/s11814-013-0176-7

pISSN: 0256-1115
eISSN: 1975-7220

Effects of discrete source-sink arrangements on mixed convection in a square cavity filled by nanofluid

Mohsen Izadi*†, Amin Behzadmehr, and Mohammad Mohsen Shahmardan***

*Mechanical Engineering Department, Shahrood University of Technology, P. O. Box 3619995161-316 Shahrood, Iran
**Mechanical Engineering Department, University of Sistan and Baluchestan, P. O. Box 98164-161 Zahedan, Iran
(*Received 2 May 2013 • accepted 12 September 2013*)

Abstract−Laminar mixed convection of Al_2O_3/water nanofluid flow in a cavity in which the upper wall is moving from right to left has been studied numerically. Fifteen different arrangements of two discrete sources and four discrete sinks have been considered. This work shows when one source is located at the right side of the bottom wall and other one at the down half of the left wall, total heat transfer achieves its maximum value. The lowest heat transfer rate is achieved when more than two vortexes are created in the cavity (case 13 for Ri=1 and case 5 for Ri=100). In general, for cases with one overall vortex, the cavities which have separate sources induce better cooling and have higher Nu number.

Keywords: Nanofluid, Discrete Source-sink, Heat Transfer Enhancement, Laminar Mixed Convection, Cavity

INTRODUCTION

Researchers and engineers are extensively seeking to find new ways to respond to industrial demands in the area of advanced thermal sciences. Using heat transfer fluids with superior thermal properties compared to the conventional one could be a historical progress on the heat transfer enhancement. Maxwell's idea of using metallic millimeter or micrometer-sized particles to enhance the thermal conductivity of fluid is well known [1]. However, such particles could not be used because of some problems such as abrasion and clogging. Modern technology provides great opportunities to produce materials with average size of 100 nm and less. These particles could be well dispersed in the conventional heat transfer fluid such as water, ethylene glycol (EG) and oil to produce a new kind of heat transfer fluid called nanofluid [2]. Miniaturization trends at different industries could be said to strongly depend on the thermal management of the devices. Nanofluid as a novel heat transfer fluid could play an important role to improve thermal efficiency of devices such as heat exchangers and cooling systems. Using different models, many numerical studies have been done to consider hydrodynamics and thermal behavior of nanofluid flow. Izadi et al. [3] numerically showed when the order of magnitude of heating energy is much higher than the momentum energy, then the friction coefficient depends on the nanoparticle concentration under laminar forced convection of Al_2O_3/water nanofluid flowing in an annulus. Also, at higher Reynolds numbers for which the momentum energy increases, this dependency on the nanoparticle volume fraction decreases. Moreover, in a recent work on the mixed convection of nanofluid through an annulus, Izadi et al. [4] demonstrated that the dimensionless axial velocity is slightly increased at the top side of the annulus, but it is decreased at the bottom side with respect to the volume fraction.

One of the cooling systems is heat transfer through a cavity which is extensively used for thermal management of different electronic devices. Natural convection in a cavity is one of the heat transfer mechanisms that have been studied by different researchers. Ogut [5] investigated natural convection heat transfer of water based nanofluids in an inclined square enclosure where the left vertical side is heated with a constant heat flux, the right side is cooled, and the other sides are kept adiabatic. His results show that the average heat transfer rate significantly increases as particle volume fraction and the Rayleigh number increase. The results also show that the length of the heater is also an important parameter affecting the flow and temperature fields. Lage and Bejan [6] investigated the buoyancy driven flows in a square enclosure with periodic heat flux. They studied the effects of oscillation frequency of heat generation on natural convection. Other researchers examined similar studies for a pure fluid within the enclosure (Kwak et al. [7], Kwak et al. [8] Kazmierczak et al. [9], Kazmierczak et al. [10]). Ghasemi et al. [11] examined the periodic natural convection in an enclosure filled with nanofluids. In their study, while a heat source with oscillating heat flux was located on the left wall of the enclosure, the right wall was maintained at a relatively low temperature and the other walls were thermally insulated.

Alloui et al. [12] did an analytical and numerical study of natural convection in a shallow rectangular cavity filled with nanofluids. The results were obtained from the analytical model for finite amplitude convection for which the flow and heat transfer is presented in terms of the governing parameters of the problem. Recently, Pakravan and Yaghoubi [13] studied thermophoresis of nanoparticles and the Dufour effect on natural convective heat transfer of nanofluids simultaneously.

Researchers and engineers have been remarkably paying attention to mixed convection heat transfer in the enclosures because of its practical importance. Mixed convection in cavity lid driven has a wide range of engineering and industrial applications such as solar power collectors, cooling of radioactive waste containers, electronic

†To whom correspondence should be addressed.
E-mail: m.izadi@mech.tus.ac.ir, m.izadi.mec@gmail.com
Copyright by The Korean Institute of Chemical Engineers.

equipment cooling, and so on. Mixed convection occurs when both the natural convection and forced convection are significant and must simultaneously be considered. Tiwari and Das [14] studied the heat transfer augmentation in a two-sided lid-driven differentially heated square cavity utilizing nanofluids. They found that both the Richardson number and the direction of the moving walls affect the fluid flow and heat transfer in the cavity. Kahveci [15] investigated the buoyancy driven heat transfer of water-based nanofluids in a differentially heated, tilted enclosure. Muthtamilselvan et al. [16] numerically studied the transport mechanism of mixed convection in a lid-driven enclosure filled with nanofluids. They showed that the heat transfer coefficient of a nanofluid augments with the nanoparticle concentration. Jahanshahi et al. [17] investigated heat transfer enhancement in a square cavity subject to different side wall temperatures using water/SiO_2 nanofluid.

In the present work, the effect of discrete source-sink arrangements of the cavity, which is filled by a nanofluid, on the cooling performance has been studied. The thermal and hydrodynamic indexes are investigated and discussed to achieve the best thermal condition. Since nanoparticles are very small, they are easily dispersed and can be approximately considered to behave as a homogeneous fluid (Xuan et al. [18]). Thus, a single phase approach is reasonably sound to use in such conditions (Yang et al. [19]). Using this formulation and geometrical configurations, the effects of nanoparticle volume fraction on the thermo-fluid parameters are investigated.

PROBLEM DEFINITION AND MATHEMATICAL MODELING

Fig. 1 illustrates details of the present problem configuration and corresponding boundary conditions. Laminar mixed convection of Al_2O_3/water nanofluid inside a lid driven cavity, of which its top wall moves while other ones are stationary, has been studied in order to achieve the best cooling condition. Influence of arrangement of four sinks and two sources, volume fraction of nanoparticles and Richardson number on thermal parameter of nanofluid flow are investigated. The top wall is considered adiabatic while thermal conditions of the other walls are varied for different considered cases. Density, viscosity and thermal conductivity of nanofluid are considered as a function of temperature while other physical properties are assumed to be constant. Both of phases are in thermal and hydrodynamic equilibrium so that there is no slip temperature and velocity between them. However, the influence of buoyancy forces is taken into account while dissipation effects are negligible.

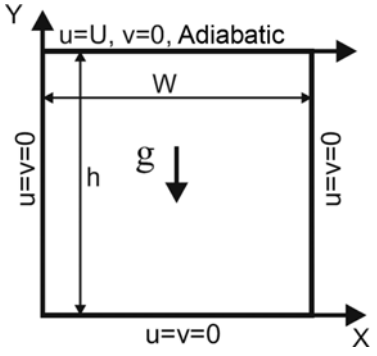

Fig. 1. Geometry of present problem.

Regarding the above assumptions, a set of nonlinear elliptical conservative governing equations under two-dimensional, laminar mixed convection, steady state and incompressible nanofluid flow follow:

Continuity:

$$\nabla\cdot(\rho_{eff}\mathrm{V}_m)=0 \tag{1}$$

Momentum:

$$\nabla\cdot(\rho_{eff}\mathrm{V}_m\mathrm{V}_m)=-\nabla\mathrm{p}+\nabla\cdot(\tau)-\rho_{eff,c}\beta_{eff}(\mathrm{T}-\mathrm{T}_c)\mathrm{g} \tag{2}$$

Energy:

$$\nabla\cdot(\rho_{eff}\mathrm{c}_{eff}\mathrm{V}_m\mathrm{T})=\nabla\cdot(\mathrm{k}_{eff}\nabla\mathrm{T}) \tag{3}$$

Where

$$\tau=\mu_{eff}\nabla\mathrm{V}_m \tag{4}$$

The physical properties in the present work are defined as following:

Effective density:

$$\rho_{eff}=(1-\varphi)\rho_f+\varphi\rho_p \tag{5}$$

An accurate equation is used for calculating the effective heat capacitance:

$$\mathrm{c}_{eff}=\frac{(1-\varphi)\rho_f\mathrm{c}_f+\varphi\rho_p\mathrm{c}_p}{\rho_{eff}} \tag{6}$$

The Chon et al. [20] correlation, which takes into account the Brownian motion and mean diameter of the nanoparticle, has been used for calculating the effective thermal conductivity:

$$\frac{\mathrm{k}_{eff}}{\mathrm{k}_f}=1+64.7\times\varphi^{0.7460}\left(\frac{\mathrm{d}_f}{\mathrm{d}_p}\right)^{0.3690}\left(\frac{\mathrm{k}_s}{\mathrm{k}_f}\right)^{0.7476}\times\mathrm{Pr}^{0.9955}\times\mathrm{Re}^{1.2321} \tag{7}$$

Where Pr and Re in Eq. (7) are defined as

$$\mathrm{Pr}=\frac{\mu}{\rho_f\alpha_f}$$

$$\mathrm{Re}=\frac{\rho_f\mathrm{B}_c\mathrm{T}}{3\pi\mu^2 l_{bf}}$$

L_{bf} is the mean free path of water, B_c is Boltzmann constant (1.3807×10^{-23} j/k) and is calculated by the following equation:

$$\mu=\mathrm{A}\times10^{\frac{B}{T-C}},\ \mathrm{C}=140,\ \mathrm{B}=247,\ \mathrm{A}=2.414\mathrm{e}-5$$

Masoumi et al. [21] developed a new equation for prediction of the nanofluids effective viscosity that is a function of temperature, mean nanoparticle diameter, nanoparticle volume fraction, nanoparticle density and the based fluid physical properties. This equation is adopted for calculating nanofluid effective viscosity:

$$\mu_{eff}=\mu_f+\mu_{app} \tag{8}$$

where μ_f and μ_{app} are base fluid and apparent viscosity, respectively. Apparent viscosity is defined by:

$$\mu_{app}=\frac{\rho_p\nu_B\mathrm{d}_p^2}{72\delta\mathrm{c}}$$

where c depends on the base fluid viscosity and mean diameter of the nanoparticle, δ depends on mean diameter and volume fractions of the nanoparticle and ν_B is the Brownian velocity of nano-

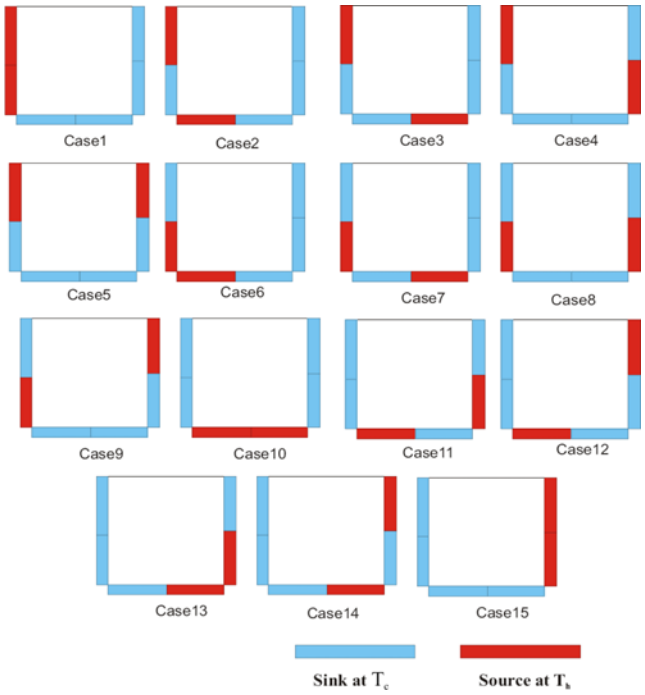

Fig. 2. Different cases of present problem.

particle that depends on temperature, diameter and density of particle.

Thermal expansion coefficient (Khanafer et al. [22]):

$$\beta_{eff}=\left[\frac{1}{1+\frac{(1-\varphi)\rho_f\beta_f}{\varphi\rho_p}}\frac{\beta_p}{}+\frac{1}{1+\frac{\varphi\rho_p}{(1-\varphi)\rho_f}}\right]\beta_f \tag{9}$$

1. Boundary Condition and Parameter Definitions

Left and right vertical walls: u=v=0

Bottom horizontal wall: u=v=0

Upper horizontal wall: $u=U_0$, v=0 and $\partial\theta/\partial y=0$

The thermal boundary condition of bottom and side walls has been adopted according to different cases (Fig. 2). A streamline has been used to depict the flow pattern and heat transfer process. Stream function (ψ) is defined in terms of continuity equation as

$$\frac{\partial\psi}{\partial Y}=U,\ -\frac{\partial\psi}{\partial X}=V$$

To calculate the heat transfer enhancement and finally optimum heat transfer under possible arrangement of source-sinks, the average Nusselt number at the source and sink is calculated based on the following equation:

$$Nu=\int_{surface}\left(-\frac{\partial T}{\partial X}\right)d. \tag{10}$$

Table 1. Grid dependency test (Gr=10,000, Re=10)

Number of nodes in x-y	Nu_{bw}	Nu_{rw}	Nu_{lw}
80*80	9.568	3.831	3.737
100*100	9.569	3.833	3.739
130*130	9.57	3.833	3.74

Dimensionless variables are defined as follows:

$$X=\frac{x}{W},\ Y=\frac{y}{H},\ \theta=\frac{T-T_c}{T_h-T_c},\ Re=\frac{U_oH}{\nu},\ Gr=\frac{g\beta(T_h-T_c)H^3}{\nu^2}$$

NUMERICAL METHOD AND VALIDATION

A set of nonlinear elliptical governing equations has been solved numerically using finite volume method on staggered grids. Diffusion terms have been discretized by central difference scheme while a hybrid difference scheme is adopted for the convective terms. Tridiagonal matrix algorithm has been used to solve discretized equations. The SIMPLE algorithm has been used for pressure-velocity coupling. A grid independence test has been performed to find suitable grid numbers for which the hydrodynamic and thermal parameters have not been significantly changed. Thus, the selected grid for this study is 100×100. Table 1 shows some of the results obtained for the grid test. To see the precision and accuracy of the results, comparisons with the results of Basak et al. [23] have been done for case 10. As seen in Table 2 good agreement between the results is obtained. Thus, the simulation code is reliable and could predict the flow behavior with a good precision.

RESULTS AND DISCUSSION

Effects of different arrangements of source-sink, concentration of nanoparticles and Richardson numbers of a lid driven cavity which is filled by Al_2O_3/water nanofluid on the rate of heat transfer were studied numerically. Thus the effect of discrete source-sink arrangements, located on bottom and sidewalls, were considered while nanoparticle volume fraction was held at 3%. Then, for the arrangement leading the best heat transfer rate, concentration of nanoparticles was changed from 0 up to 5% for two different Richardson numbers (1 and 100). Finally, for a given Reynolds number (10), effect of Ri on the rate of heat transfer was studied. For a given Ri=1, Fig. 3 shows streamlines of nanofluid flow in the cavity for different arrangement of source-sink. As observed for case 1, there is overall a clockwise vortex in the cavity. At the left corner of the bottom wall, the buoyancy force which arises from case 2 creates a small vortex which circulates nanofluid flow between source and sink. This could enhance the rate of heat transfer. For the next case (c), despite the growing vortex, it is not effective because of circulating nanofluid between two sinks. On the other hand, the effect of overall

Table 2. Comparison of predicted Nusselt number with Basak et al. at Gr=10,000 and Pr=10

Nu (average Nusselt number)									
	Bottom wall			Right wall			Left wall		
Gr	Present	Basak et al.	Error	Present	Basak et al.	Error	Present	Basak et al.	Error
100000	9.56879	9.028	0.059901	3.8319	4.30435	0.10979	3.7372732	4.02341	0.07112

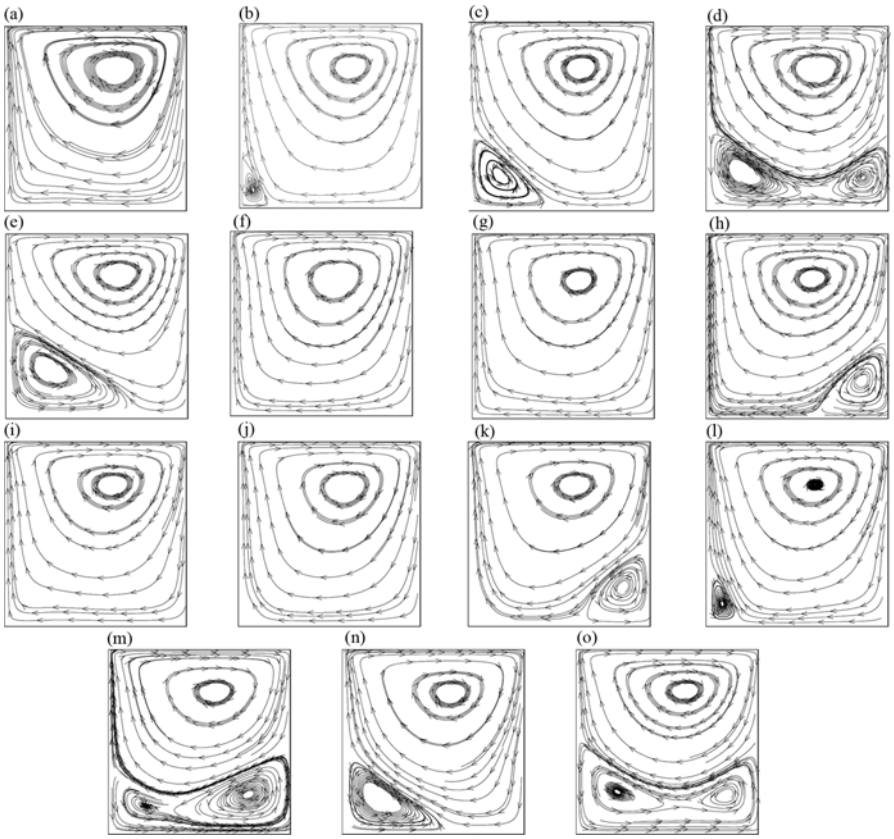

Fig. 3. Streamlines for different source-sink arrangement cases at Ri=1: (a) case 1 (b) case 2 (c) case 3 (d) case 4 (e) case 5 (f) case 6 (g) case 7 (h) case 8 (i) case 9 (j) case 10 (k) case 11 (l) case 12 (m) case 13 (n) case 14 (o) case 15.

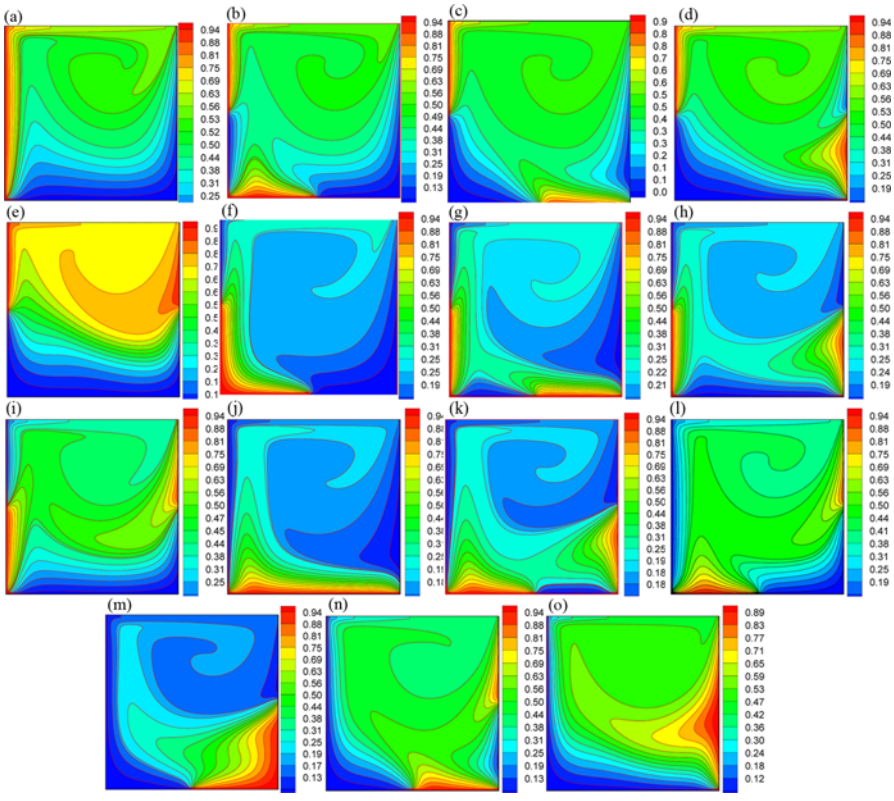

Fig. 4. Isotherms and distribution of dimensionless temperature (θ) for different cases at Ri=1: (a) case 1 (b) case 2 (c) case 3 (d) case 4 (e) case 5 (f) case 6 (g) case 7 (h) case 8 (i) case 9 (j) case 10 (k) case 11 (l) case 12 (m) case 13 (n) case 14 (o) case 15.

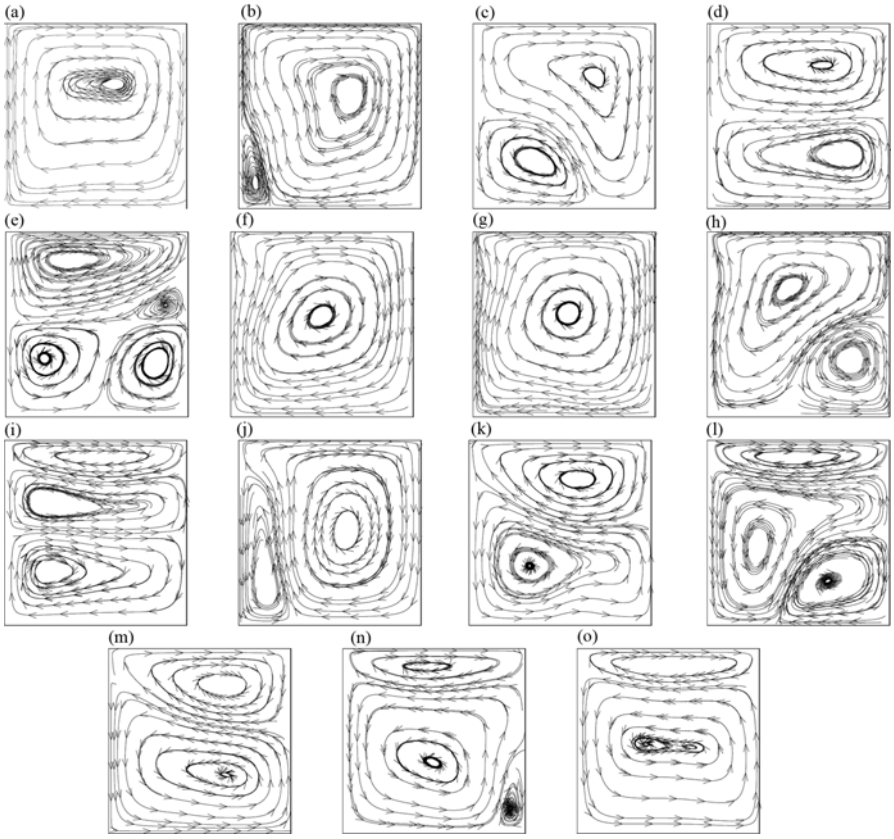

Fig. 5. Streamlines for different cases for Ri=100: (a) case 1 (b) case 2 (c) case 3 (d) case 4 (e) case 5 (f) case 6 (g) case 7 (h) case 8 (i) case 9 (j) case 10 (k) case 11 (l) case 12 (m) case 13 (n) case 14 (o) case 15.

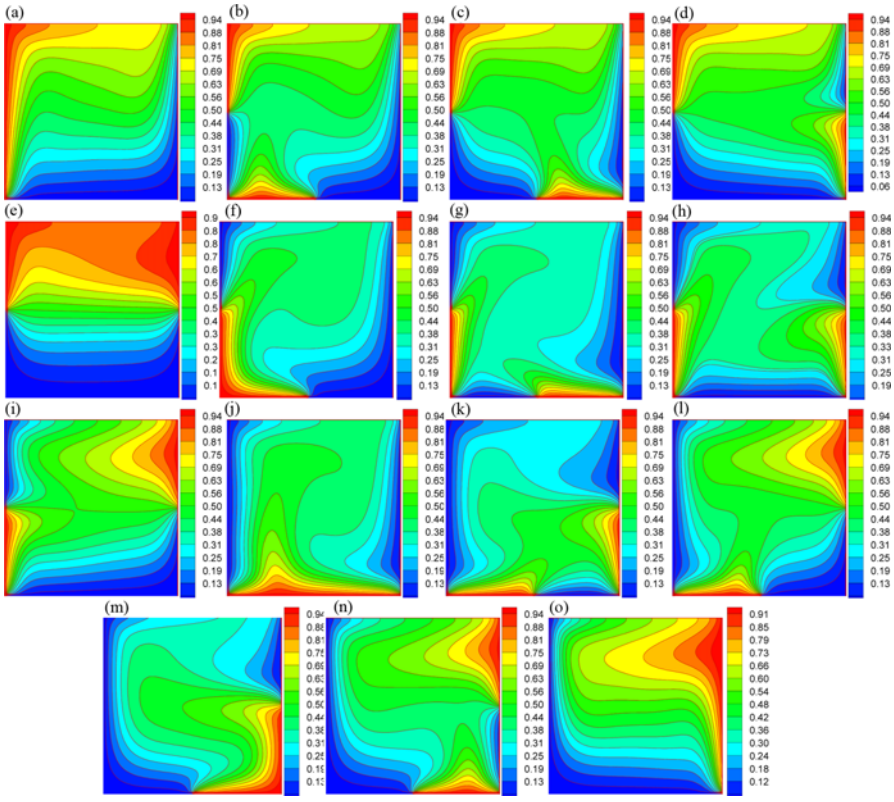

Fig. 6. Isotherms and distribution of dimensionless temperature (θ) for different cases at Ri=100: (a) case 1 (b) case 2 (c) case 3 (d) case 4 (e) case 5 (f) case 6 (g) case 7 (h) case 8 (i) case 9 (j) case 10 (k) case 11 (l) case 12 (m) case 13 (n) case 14 (o) case 15.

vortex becomes less important. This situation continues up to the case 5. For this case, warm nanofluid flow cannot be cooled by sinks at the bottom wall due to presence of a small vortex, which deteriorates streamlines of the main vortex. For case 6, the main (overall) vortex circulates nanofluid throughout the cavity. Under such circumstances, buoyancy forces intensify the inertial ones. Although there is an overall vortex for cases 6 and 7, better heat transfer is expected for case 7. Case 7 separates sources, each of which is cooled by its neighbor sink. Althouth for case 8, bouyancy forces create a small vortext at the right side of bottom wall; it circulates nanofluid flow between one pair of source-sink at the right corner of bottom wall, which is expected to enhance heat transfer from the right wall and also is reduced at the left one. For two later cases, one vortex circulates flow between source and sinks. Cases 11 and 12 are similar to case 8 and an inferior vortex exists between a pair of source-sink. Two small vortices strongly can increase the heat transfer coefficient. For case 13, the position of vortices which circulate nanofluid between two sources at right and two sinks at left have negetive effect on the rate of heat transfer. This situation not only directly decreases heat transfer between the pair of the source-sinks but also deteriorates the effect of the main (overall) vertex. At the next case (case 14), two subsidiary vortices reduce to one, leading to better heat transfer. Though a similar flow pattern of the case 13 can be observed at the case 15, one of subsidiary vortices that is located at right corner circulates flow between a pair of source-sinks. In this case, better heat transfer would be expected compared to the case 13. In general, the cavities which have separate sources induce better cooling and have higher Nu number (cases 2, 7, 9 and 12). The lowest Nu number is achieved for the cavities which have more than one vortex (cases 5 and 13). The walls for which two sources are located there have higher rate of heat transfer compared to other walls (cases 1, 10 and 15). Fig. 4 shows the distribution of temperature at different cases. It is clearly observed that some cases whose temperature distribution is more uniform have better cooling condition. In case 7, accumulation of warmer nanofluid is seen at the region near the sources while the cooler fluid is served at the near sinks region. A cooler region near the bottom and right walls in which two sinks are located is observed (cases 1, 4, 5, 8, 9, 15 for bottom wall). But such cooler nanofluid does not exist in the region near the wall that contains two sinks. This arises from the fact that the main vortex which is created by upper moving wall carries warm nanofluid to the near of the left wall. The flow pattern is presented for Ri=100 in Fig. 5. As seen, streamlines completely are different from those for Ri=1. The bouyancy forces become stronger. In general, they create bigger and more effective vortices. Howevere, two bottom vortices of case 5 circulate nanofluid between sinks while upper (main) vortex circulates fluid between sources. It is clear that this pattern could not serve as a proper cooling condition. However, some vortices which circulate nanofluid between both of source and sink could enhance the rate of heat transfer (cases 8 and 11), and some other which circulates between either sources or sinks decreases the rate of heat transfer (case 5). As seen in Fig. 6 for Ri=100, for some cases, warmer nanofluid accumulates at the region near the sorces and the cooler fluid near the sinks (cases 5, 9 and 15). Therefore,

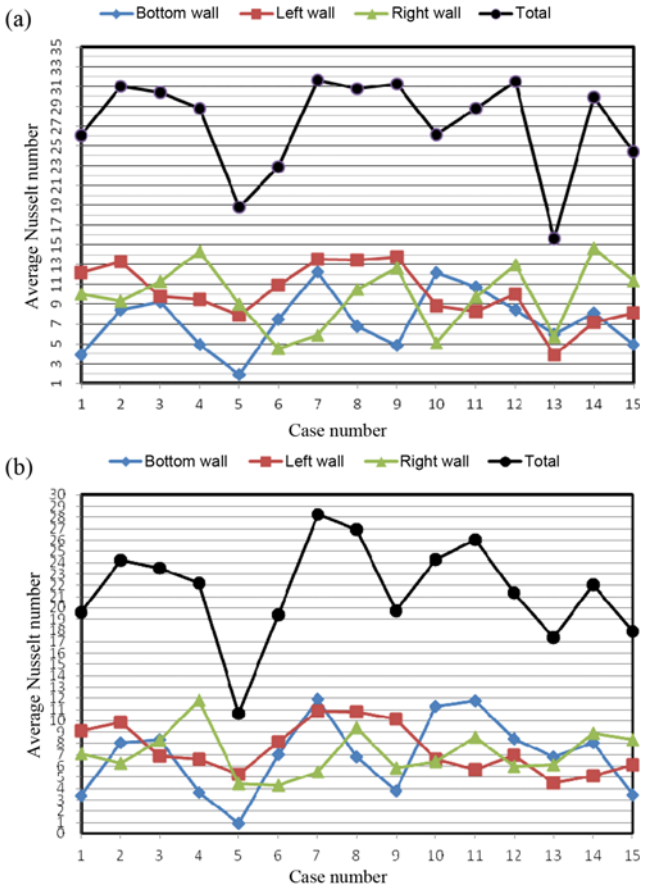

Fig. 7. Average Nusselt number for different cases: (a) Ri=1 (b) Ri=100.

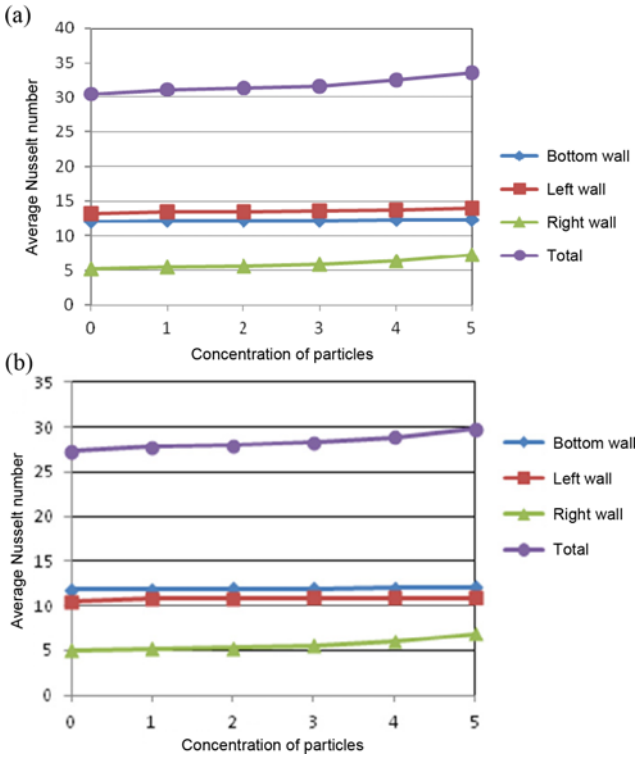

Fig. 8. Average Nusselt Number against concentration of particles (a) (Ri=1) (b)(Ri=100).

the uniformity of temperature distribution deteriorates in these cases. At some cases, the flow is well mixed by forced and bouyancy forces so that uniform temperature distribution is achieved (cases 7, 8, 10 and 11). Fig. 7 shows the variation of average Nusselt number with respect to different cases for two Ri. Higher total heat transfer rate is seen in case 7 for both Ri. While, the least Nu occurs in the cavities which have less uniform temperature distribution and more than one vortex (cases 5, 13 and 15). The high Nu are achieved in the cavities which either have one main vortex or the small vortex circulates nanofluid between source-sink(s) (cases 2, 7, 8, 9, 12 for Ri=1 and cases 7 and 8 for Ri=100). As shown in Fig. 8, nanoparticle concentration slightly affected the total average Nusselt number, while it does not have any significant effect on the left and bottom wall average Nusselt number. The streamline structure is shown in Fig. 9 for different Ri. The buoyancy forces displace streamlines toward the bottom of the cavity. The effect of this variation on the temperature distribution is shown in Fig. 10. Buoyancy forces which augment with an increase in Ri cause more uniformity on the temperature distribution. This means more energy transfers through the nanofluid.

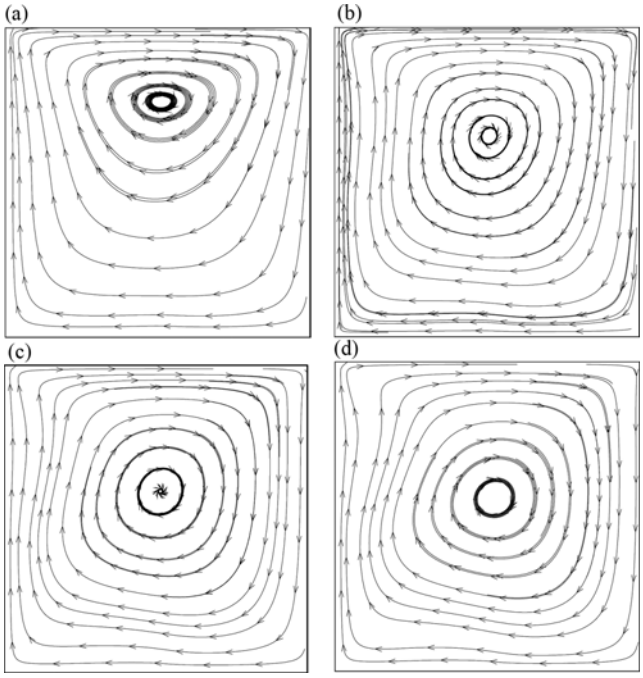

Fig. 9. Streamlines for different Richardson number at φ=3%: (a) Ri=10 (b) Ri=40 (c) Ri=70 (d) Ri=100.

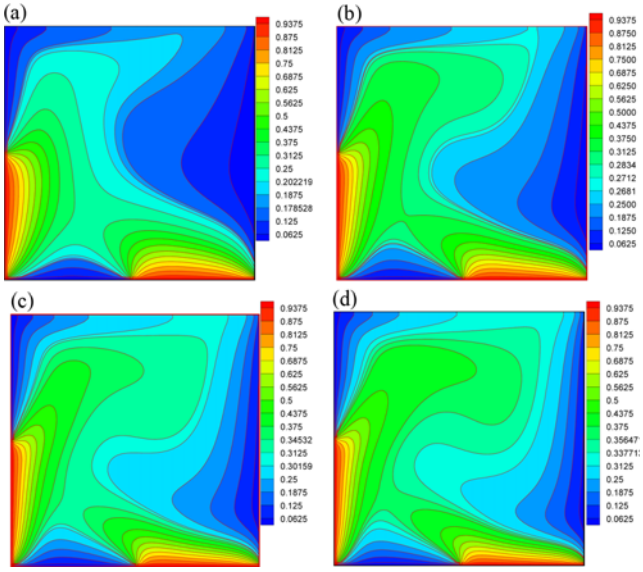

Fig. 10. Isotherms and distribution of dimensionless temperature (θ) for different Richardson number at φ=3%: (a) Ri=10 (b) Ri=40 (c) Ri=70 (d) Ri=100.

CONCLUSION

From our investigation of the effect of discrete source-sink arrangements on the thermal performance of a cavity filled by a nanofluid, the results can be summarized as follows:

[1] The cavities which have separate sources provide better cooling and have higher Nu (cases 2, 7, 9 and 12).

[2] The highest rate of heat transfer is achieved for the case 7 for which one overall vortex circulates.

[3] The lowest heat transfer rate is achieved when more than two vortexes are created in the cavity (case 13 for Ri=1 and case 5 for Ri=100).

[4] The wall in which two sources are located nearby has higher rate of heat transfer compared to the other walls.

[5] In general, for higher Ri, the bouyancy forces create more effective vortices in the cavity.

[6] In none of cases, the bottom wall has the maximum Nu number.

[7] When two sinks are located at the left wall, the right or bottom wall has the maximum Nu compared to other walls.

[8] When two sinks are located at the bottom wall, the right or left wall has the maximum Nu compared to the other walls.

[9] At low Ri number, 1-10, rate of heat transfer sharply decreases with an increase in Ri, but it increases slightly at the higher value of Ri number (10-100).

[10] In general, nanoparticle concentration slightly increases the total average Nusselt number, while it does not have any significant effect on the left and bottom wall average Nusselt number.

NOMENCLATURE

A, B, C : constant
B_c : Boltzmann constant
C_p : specific heat at constant pressure [J/kgK]
d : with or height of the cavity [H or W]
d_f : molecular diameter of base fluid
d_p : nanoparticle diameter [nm]
f : fluid
g : gravitational acceleration [ms^{-2}]
h : heat transfer coefficient
H : height of the cavity
k : thermal conductivity [W/mK]
L_{bf} : mean free path of base fluid
Nu : Nusselt number
P : pressure

Pr : Prandtl number
Re : Reynolds number
s : solid
S : x or y coordinate
T : temperature
u : velocity in x direction [m/s]
v : velocity in y direction [m/s]
V : velocity [m/s]
v_B : brownian motion
W : with of the cavity
X : dimensionless x-coordinate
xvx-coordinate
Y : dimensionless y-coordinate
y : y-coordinate

Greek Letter

μ : dynamic viscosity [pa·s]
ν : kinematic viscosity [m^2s^{-1}]
θ : dimensionless temperature
τ : shear stress [pa]
φ : volume fraction

Subscripts

app : appearance
av : average
b : bottom
c : cool
eff : effective
h : hot
l : left
m : mixture
p : particle
r : right
w : wall

REFERENCES

1. J. C. Maxwell, *A treatise on electricity and magnetism*, Clarendon Press (1891).
2. S. U. S. Choi, *Enhancing thermal conductivity of fluid with nanoparticles, developments and applications of non-Newtonian flow*, ASME FED 231/MD 66, 99 (1995).
3. M. Izadi, A. Behzadmehr and D. Jalali-Vahid, *Int. J. Therm. Sci.*, **48**, 2119 (2009).
4. M. Izadi, M. M. Shahmardan, M. J. Maghrebi and A. Behzadmehr, *Chem. Eng. Commun. 723077*, **200**(7) (2013).
5. E. B. Ogut, *Int. J. Therm. Sci.*, **48**, 2063 (2009).
6. J. L. Lage and A. Bejan, *Int. J. Heat Mass Transf.*, **36**(8), 2027 (1993).
7. H. S. Kwak and J. M. Hyun, *J. Fluid Mech.*, **329**, 65 (1996).
8. H. S. Kwak, K. Kuwahara and J. M. Hyun, *Int. J. Heat Mass Transf.*, **41**(18), 2837 (1998).
9. M. Kazmierczak and Z. Chinoda, *Int. J. Heat Mass Transf.*, **35**(6), 1507 (1992).
10. M. Kazmierczak and A. Muley, *Int. J. Heat Fluid Flow*, **15**(1), 30 (1994).
11. B. Ghasemi and S. M. Aminossadati, *Int. J. Therm. Sci.*, **49**, 1 (2010).
12. Z. Alloui, P. Vasseur and M. Reggio, *Int. J. Therm. Sci.*, **50**(3), 385 (2011).
13. H. A. Pakravan and M. Yaghoubi, *Int. J. Therm. Sci.*, **50**(3), 394 (2011).
14. R. K. Tiwari and M. K. Das, *Int. J. Heat Mass Transfer*, **50**(9-10), 2002 (2007).
15. K. Kahveci1, *J. Heat Transfer*, **132**(6), 062501-129 (2010).
16. M. Muthtamilselvana, P. Kandaswamya and J. Lee, *Communications in Nonlinear Science and Numerical Simulation*, **15**(6), 1501 (2010).
17. M. Jahanshahi, S. F. Hosseinizadeh, M. Alipanah, A. Dehghani and G. R. Vakilinejad, *Int. Commun. Heat Mass Transfer*, **37**(6), 687 (2010).
18. Y. Xuan and Q. Li, *Int. J. Heat Fluid Flow*, **21**, 58 (2000).
19. Y. Yang, Z. G. Zhang, E. A. Grulke, W. B. Anderson and G. Wu, *Int. J. Heat Mass Transf.*, **48**, 1106 (2005).
20. C. H. Chon, K. D. Kihm, S. P. Lee and S. U. S. Choi, *Appl. Phys. Lett.*, **87**, 1 (2005).
21. N. Masoumi, N. Sohrabi and A. Behzadmehr, *J. Phys. D: Appl. Phys.*, **42**, 055501 (2009).
22. K. Khanafar, K. Vafai and M. Lightstone, *Int. J. Heat Mass Transf.*, **46**, 3639 (2003).
23. T. Basak, S. Roy, P. K. Sharma and I. Pop, *Int. J. Therm. Sci.*, **48**, 891 (2009).